

## Sigma-0 Retrieval from SeaWinds on QuikSCAT

Ivan S. Ashcraft<sup>a</sup>, David G. Long<sup>a</sup>, Arden Anderson<sup>a</sup>  
Steve Richards<sup>a</sup>, Mike Spencer<sup>b</sup>, Brian Jones<sup>a</sup>

<sup>a</sup>Brigham Young University, Provo, Utah, U.S.A.

<sup>b</sup>Jet Propulsion Laboratory, 4800 Oak Grove Drive, Pasadena, California 91109, U.S.A.

### ABSTRACT

NASA has developed a new scatterometer, *SeaWinds*, which is scheduled to be launched on two missions, one in 1999 and the other in 2000. *SeaWinds* will measure the speed and direction of near-surface winds over the ocean. A fundamental part of the processing of *SeaWinds* data is the computation of  $\sigma^o$  which includes solving the radar equation<sup>1</sup> for every pulse sent and received by the scatterometer. However, for *SeaWinds*, this calculation is too computationally intensive to perform in real time. Instead, a method of tabularizing most of the calculation has been developed. This method includes corrections for attitude and orbit perturbations and accounts for the elevation of the local topography. It also includes a table which will be used to assist ground data processing in determining the locations of the measurements. Tests comparing the tabulated results with the actual numerical calculations have shown that using this table is accurate to within  $\pm 0.1$  dB and gives locations that are accurate to within 160 meters. We provide a description of this algorithm. The innovations developed as part of this algorithm may be of interest in processing data from other remote sensing systems.

**Keywords:** Scatterometer, *SeaWinds*, *QuikSCAT*, ADEOS II, NSCAT, ocean winds, radar equation, sigma-0

### 1. INTRODUCTION

A new scatterometer, *SeaWinds*, has been developed by NASA as part of the Earth Observing System (EOS). *SeaWinds* will measure the normalized radar backscatter ( $\sigma^o$ ) of the Earth's surface. The  $\sigma^o$  measurements made by *SeaWinds* will be used for multiple global climate and environmental studies. The primary use of the measurements is in determining the speed and direction of the near-surface winds over the ocean. Over 90% of the ocean's surface will be covered each day. Because winds modulate all air-sea fluxes, this data will be important in weather prediction and air-sea interaction studies. The measurements will also be used to produce images of the rain-forests, the polar ice caps, and other areas of the Earth at microwave frequencies. These images will be used to analyze large scale changes in the Earth's environment. *SeaWinds* is currently scheduled for two missions: *SeaWinds* on *QuikSCAT*, and *SeaWinds* on *ADEOS II*. *QuikSCAT* will be launched in June 1999 as a replacement for the *NASA Scatterometer* (NSCAT). ADEOS II is scheduled for launch during November 2000.

*SeaWinds* has a pencil beam design rather than the fan-beam design of previous spaceborne scatterometers such as NSCAT. *SeaWinds* transmits 13.4 GHz microwave pulses at a pulse rate of 200 Hz using a rotating dish antenna. The radar transmits two beams, one horizontally polarized and the other vertically polarized. These beams trace out a helix on the earth as the satellite passes overhead. Using the returned power from each transmitted pulse, the average  $\sigma^o$  value of the illuminated area is calculated. For each pulse, each beam illuminates an elliptical area on the Earth's surface referred to as an "egg." *SeaWinds* uses a chirped signal and a digital processor for range filtering to divide this egg into 12 "slices." The digital processor has 8 different operational modes which adjust the width of the slices. Figure 1 shows the 3 dB contours of the egg and the slices for a typical measurement.

Because of the characteristics of the pencil-beam geometry employed by *SeaWinds*, the integral form of the radar equation<sup>1</sup> must be used to obtain  $\sigma^o$ . This calculation is too computationally intensive to be performed in real time. Therefore, it is necessary to precalculate most of the radar equation and store it in a lookup table. This precalculated value is referred to as "X" and is related to  $\sigma^o$  through the equation

$$\sigma^o = \frac{P_r}{X}, \quad (1)$$

---

Correspondence:

I.S.A.: E-mail: ashcraft@ee.byu.edu

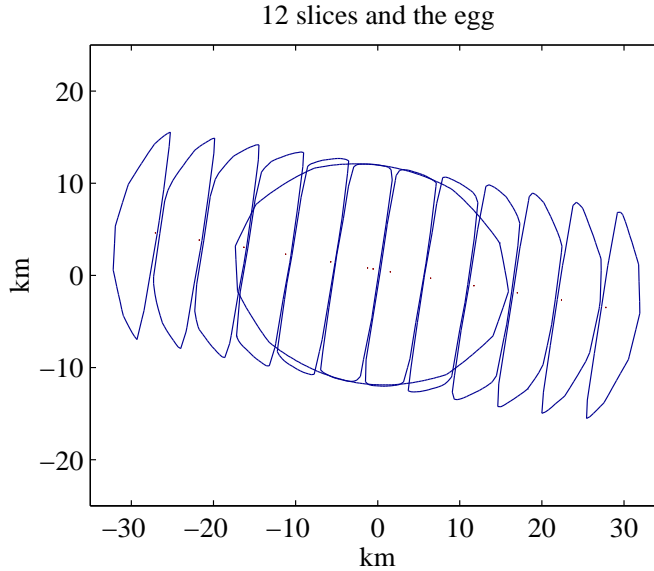


**Figure 1.** The 3 dB contours of the “egg” and 12 “slices” for a typical *SeaWinds* measurement plotted on a kilometer grid.

where  $P_r$  is the return power.

In order to minimize the error in the  $\sigma^\circ$  measurements,  $X$  is required to be accurate to within  $\pm 0.1$  dB. To achieve this accuracy, the X-table must include a way to compensate for satellite perturbations. We have developed an algorithm that includes a table of nominal  $X$  values and a method to correct these values for the expected perturbations. The algorithm also includes a correction for the elevation of the local topography and a tabularization of the slice centers. The elevation correction will result in more accurate  $\sigma^\circ$  measurements over land, and the slice center table will help simplify the ground data processing for *SeaWinds*.

## 2. $X$ AND THE RADAR EQUATION

The average  $\sigma^\circ$  value over a slice can be calculated using the integral form of the radar equation. For the discrete case (which must be used for numerical integration) the integral form of the radar equation from Ulaby et al.<sup>1</sup> is

$$P_r = \frac{\lambda^2}{(4\pi)^3} \sum_{i \in \mathcal{F}} \frac{P_{t,i} G_i^2 \sigma^\circ \delta A_i}{R_i^4} \quad (2)$$

where  $P_r$  is the average received power,  $\lambda$  is the wavelength,  $\mathcal{F}$  is the illuminated area,  $P_{t,i}$  is the power illuminating each incremental area ( $\delta A_i$ ),  $G_i$  is the gain over each incremental area, and  $R_i$  is the slant range from the satellite to each area. Because the return signal goes through a filter bank (implemented as an FFT) for range filtering an additional term ( $G_{F,i}$ ) needs to be included so that the radar equation becomes

$$P_r = \frac{\lambda^2}{(4\pi)^3} \sum_{i \in \mathcal{F}} \frac{P_{t,i} G_i^2 \sigma^\circ \delta A_i G_{F,i}}{R_i^4}, \quad (3)$$

where  $G_{F,i}$  is the gain of the slice filter bank for the signal returned from an incremental area and  $P_r$  now represents the power returned from a single slice. The egg is defined to be the sum of the inner 10 slices. The filter gain for a particular slice is

$$G_{F,i} = \sum_{k=k_s}^{k_e} \left[ \frac{\sin^2 [\pi N_{p,i} (f_{b,i} T - (k/N))]}{\sin^2 [\pi (f_{b,i} T - (k/N))]} \right] \quad (4)$$

where  $N_{p,i}$  is the number of samples of the return signal captured by the range gate,  $f_{b,i}$  is the baseband frequency of the return signal from the incremental area,  $T$  is the sampling period,  $k_s$  and  $k_e$  are the beginning and ending frequency bins for the slice respectively, and  $N$  is the number of points in the FFT.

Using some basic assumptions, the radar equation can be solved for  $\sigma^\circ$ . First, we assume that  $\sigma^\circ$  is constant over the slice and that the power transmitted to each incremental area is constant. Using these assumptions and factoring out the peak gain ( $G_p$ ), the equation becomes

$$\bar{P}_r = \frac{\lambda^2}{(4\pi)^3} G_p^2 P_t \sigma^\circ \sum_{i=1}^N \frac{g_i^2 \delta A_i G_{F,i}}{R_i^4} \quad (5)$$

where  $P_t$  is the transmitted power and  $g_i$  is the normalized gain over each incremental area.  $P_t$  is obtained from the total energy observed in the loop-back calibration cycle ( $P_{cal}$ ) of *SeaWinds* using the equation

$$P_t = \frac{L_{cal} P_{cal}}{L_{sys} N N_{p,t}} \quad (6)$$

where  $L_{cal}$  is the loss through the loop-back path,  $L_{sys}$  is the two-way system loss,  $N$  is the number of points in the FFT, and  $N_{p,t}$  is the number of samples in the loop back signal. If we define

$$C_{cal} = \left( \frac{\lambda^2}{(4\pi)^3} \right) \left( \frac{G_p^2 L_{cal} P_{cal}}{L_{sys}} \right) \quad (7)$$

then Eq. (5) can be solved for  $\sigma^\circ$  and combined with Eq. (1) to give

$$X = \frac{C_{cal}}{N N_{p,t}} \sum_{i \in \mathcal{F}} \frac{P_{ti} g_i^2 \delta A_i G_{F,i}}{R_i^4}. \quad (8)$$

The value of  $X$  for the egg is the sum of the  $X$  values of the inner 10 slices. For the purposes of the X-table generation it is assumed that  $C_{cal} = 1$ . The correct value of  $C_{cal}$  will be included when the data is retrieved. For a complete derivation of  $X$  see Ref. 2.

### 3. TABULARIZING $X$

Because the numerical integration required to calculate  $X$  is too computationally intensive to be performed in real time, it is necessary to precalculate  $X$ , parameterize it, and enter the parameterizations into a lookup table. The method for doing this is described below.

#### 3.1. Variations in $X$ with Azimuth Angle and Orbit Time

As discussed in the previous section,  $X$  depends on the geometry of the spacecraft relative to the Earth. If the attitude and orbit of the spacecraft are known, the geometry can be calculated using the orbit time of the spacecraft\* ( $T_{orb}$ ) and the azimuth angle of the antenna ( $\phi$ ). Because  $T_{orb}$  and  $\phi$  are parameters that are known at the time the data is retrieved from the satellite, it is desirable to find a way to parameterize  $X$  as a direct function of these two parameters.

Figure 2 shows how  $X$  varies with azimuth and orbit time. Various parameterization methods were proposed for  $X(\phi, T_{orb})$  including a polynomial and a Fourier Series. The method finally chosen is a table of discrete values using linear interpolation between known points. This table contains  $X$  values for 32 values of  $T$  and 36 values of  $\phi$ . A three dimensional depiction of such a table is shown in Fig. 3. Tests have shown that the values obtained from this table are within 0.05 dB of the values obtained by directly solving Eq. (8). There is a separate table for each slice, beam, and operational mode.

#### 3.2. Including Perturbations

The major challenge in tabularizing  $X$  is finding a way to correct for possible spacecraft perturbations and quantization effects in the Range/Doppler tracking tables. A simple algorithm was finally developed.

---

\*The orbit time is defined as the time in seconds that has elapsed since the spacecraft ascended past the equator. The full orbit of the spacecraft is approximately 6060 seconds.

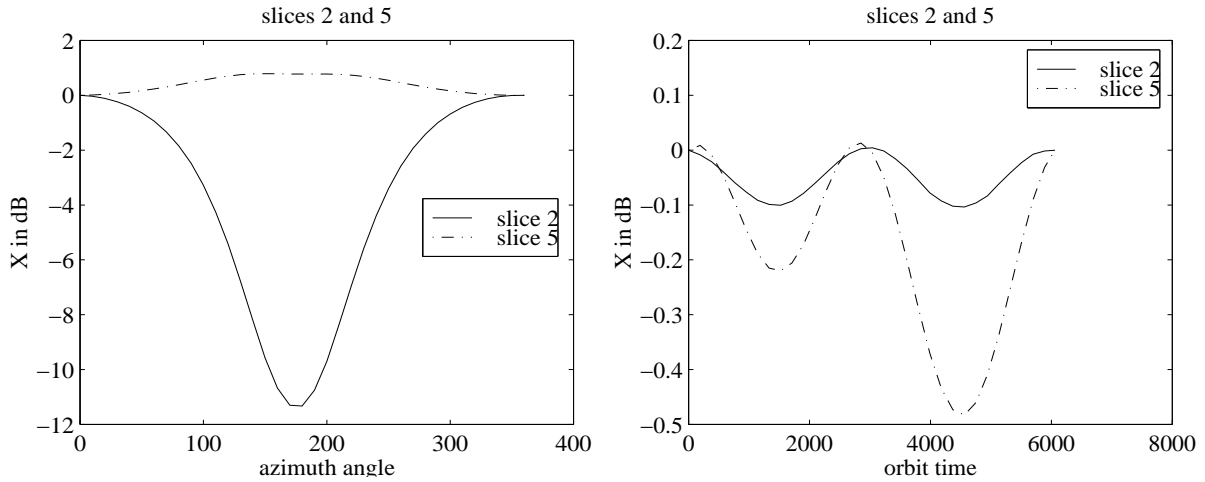


**Figure 2.** The plot on the left shows the variation of  $X$  with azimuth angle at a constant orbit time. The plot on the right shows the variation in  $X$  with orbit time for a constant azimuth angle. Both plots include slices 2 and 5.  $X$  has been normalized for easier comparison.

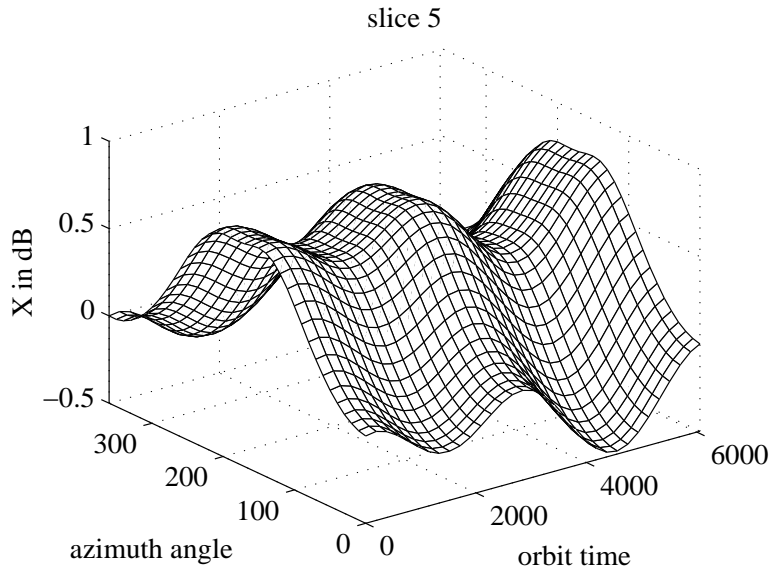


**Figure 3.**  $X$  variations over the entire orbit time and azimuth range for slice 5.  $X$  has been normalized.

There are two types of perturbations: attitude perturbations and orbit perturbations. The attitude perturbations include changes in the roll, pitch, and yaw of the spacecraft. The orbit perturbations include changes in eccentricity, the argument of perigee, and the semi-major axis. The expected perturbations for *QuikSCAT* and ADEOS II are given in Table 1.

These perturbations cause a large enough change in  $X$  that a correction to the nominal  $X$ -table is required. The method chosen to correct for perturbational errors in  $X$  uses the baseband frequency at the boresight of the antenna beam ( $\Delta f$ ) to parameterize the  $X$  correction. The nominal value of  $X$ ,  $X_{nom}$ , corrected for perturbations is  $X_{pert} = X_{nom} + \Delta X$  where  $\Delta X$  is a function of the different perturbations. Figure 4 shows a plot of  $X$  versus  $\Delta f$  for 50 different combinations of attitude and orbit perturbations. A third degree polynomial can be used to

**Table 1.** The  $3\sigma$  (3 times the standard deviation) values of the spacecraft perturbations around the nominal values assumed for *QuikSCAT* and *ADEOS II*.

parameter	QuikSCAT	ADEOS II
roll	0.1	0.3
pitch	0.1	0.3
yaw	0.1	0.3
eccentricity	$2 \times 10^{-4}$	$3 \times 10^{-5}$
arg. of per.	$10^\circ$	$2^\circ$
semi-major axis	$\approx 0$	1 km

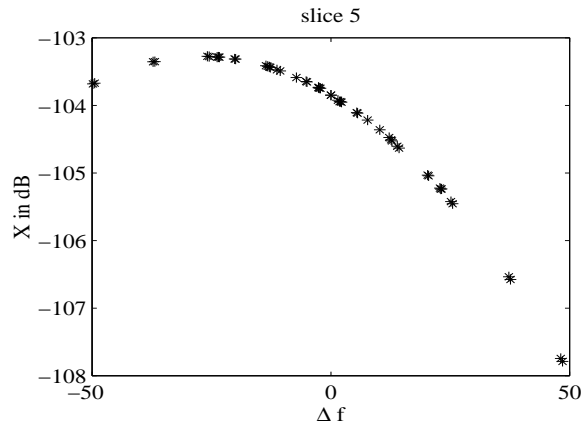


**Figure 4.** Variations in  $X$  for slice 5 using 50 different combinations of expected perturbations at a given orbit time and azimuth angle.  $X$  is plotted as a function of the baseband frequency at the boresight.

approximate  $X_{pert}$  as a function of  $\Delta f$  so that

$$X_{pert} = X_{nom} + A + B \cdot \Delta f + C \cdot \Delta f^2 + D \cdot \Delta f^3, \quad (9)$$

where  $A$  is constrained to equal zero so that for no perturbations  $X_{pert} = X_{nom}$ . The overall accuracy of  $X_{pert}$  is discussed in Sect. 5.1.

### 3.2.1. Effects of topography

Although the primary purpose of *SeaWinds* is to measure the wind over the ocean, the  $\sigma^o$  values obtained over land will also be used in many studies. Therefore, it is important to obtain accurate values of  $\sigma^o$  over the land as well as over the ocean. For measurements over land,  $X$  must be corrected for the elevation of the local topography as well as for orbit and attitude perturbations. An increase in the height of the surface is similar to a decrease in the altitude of the spacecraft, so using the  $\Delta f$  correction scheme which is used to correct  $X_{nom}$  for orbit perturbations will work for the topography elevation as well.<sup>3</sup> The relationship between topography elevation and  $\Delta f$  is linear and can be defined using the equation

$$\Delta f_{tot} = \Delta f + S \cdot h_{topo}, \quad (10)$$

where  $h_{topo}$  is the elevation of the local topography,  $S$  is the slope of the linear fit of  $\Delta f$  as a function of  $h_{topo}$ , and  $\Delta f_{tot}$  is the total frequency shift with the topography included.  $\Delta f_{tot}$  is then used in the place of  $\Delta f$  in Eq. (9).

### 3.3. Range Gate Clipping

The effects of range gate clipping have been analyzed to determine if  $X$  needs to be corrected for this factor as well. Range gate clipping occurs when a portion of the signal returned from a slice is cut off by the range gate. It was

found that range gate clipping is expected to cause  $X$  to vary by less than 0.1 dB for the inner 10 slices. The analysis included all 8 resolution modes and both beams. The analysis also showed that  $X$  is expected to vary by less than 0.02 dB for the inner eight slices for resolution modes 2 through 8, both beams. These variations are small enough that they can be ignored for the most part. However, a G-factor is included in the table in case it is later decided that the effects of range gate clipping need to be included. The equation to obtain  $X$  using the G-factor is

$$X = X_{pert} + 10 \log_{10}(G) \quad (11)$$

where  $X$  is in dB.

#### 4. TABULARIZING SLICE CENTER LOCATIONS

In order to simplify ground data processing, the elevation ( $\theta$ ) and azimuth ( $\phi$ ) angles<sup>†</sup> of the slice centers are also tabulated.<sup>4</sup> The elevation and azimuth angles of the slice centers are linear functions of  $\Delta f$  and are described by the equations

$$\begin{aligned} \phi &= \phi_o + A_\phi + B_\phi \Delta f_{tot} \\ \theta &= \theta_o + A_\theta + B_\theta \Delta f_{tot}, \end{aligned} \quad (12)$$

where  $A_\phi$ ,  $B_\phi$ ,  $A_\theta$ , and  $B_\theta$  are all precalculated using a least squares linear fit and a set of fifty perturbations.  $\theta_o$  and  $\phi_o$  are the elevation and azimuth angles, respectively, of the boresight. The coefficients of the linear fit are stored in a lookup table similar to that shown in Fig. 3 where there is a value of each for 32 orbit times and 36 azimuth angles.

#### 5. THE X-TABLE

The X-table includes all of the information required to retrieve  $X$  for the slices and egg and the slice centers for a given azimuth angle, orbit time, and  $\Delta f$ . A separate  $X$  table is generated for each beam and processor resolution mode. The variables included in the X-table are  $X_{nom}$ ,  $A$ ,  $B$ ,  $C$ , and  $D$  from Eq. (9),  $S$  from Eq. (10),  $G$  from Eq. (11), and  $A_\phi$ ,  $B_\phi$ ,  $A_\theta$ , and  $B_\theta$  from Eq. (12). Plots showing the magnitude of some of the values in the X-table and how they vary with orbit time and azimuth angle are shown in Fig. 5. For each pulse that *SeaWinds* transmits and receives, the X-table is used to obtain a value of  $X$  for the egg and all of the slices, as well as locate the slice centers. The first step in using the table is obtaining the baseband frequency at the boresight of the beam. The necessary computations are made to find  $\Delta f$  using the radius of the Earth at sea-level. Then,  $S$  is interpolated from the table and  $\Delta f_{tot}$  is calculated using Eq. (10). The value of  $X$  for the egg and each slice can then be found using Eq. (9) where  $X_{nom}$ ,  $A$ ,  $B$ ,  $C$ , and  $D$  are interpolated from the table and  $\Delta f$  is replaced with  $\Delta f_{tot}$ . The  $X$  values in the table are in dB. The slice centers can then be located using Eq. (12) where  $A_\phi$ ,  $B_\phi$ ,  $A_\theta$ , and  $B_\theta$  are all interpolated from the table and are specific to each slice. When the conversion from elevation and azimuth to latitude and longitude is made, the elevation of the local topography is included in the radius of the Earth.

##### 5.1. Accuracy

We conducted studies to determine the expected accuracy of the X-table for both *QuikSCAT* and ADEOS II.<sup>5</sup> The analysis was performed using the nominal resolution mode and included both the inner and outer beam. The maximum standard deviations for the inner 8 slices are shown in Table 2. We conclude that the X-table will meet the requirement of being accurate to within 0.1 dB for the inner 8 slices, and the slice centers will be accurate to within 160 meters.

---

<sup>†</sup>These angles are in the spacecraft coordinate system. For the spacecraft coordinate system, the azimuth angle is the angle in the plane parallel to the surface of the Earth referenced from the velocity vector of the satellite. The elevation angle is referenced from nadir, or directly below the spacecraft.

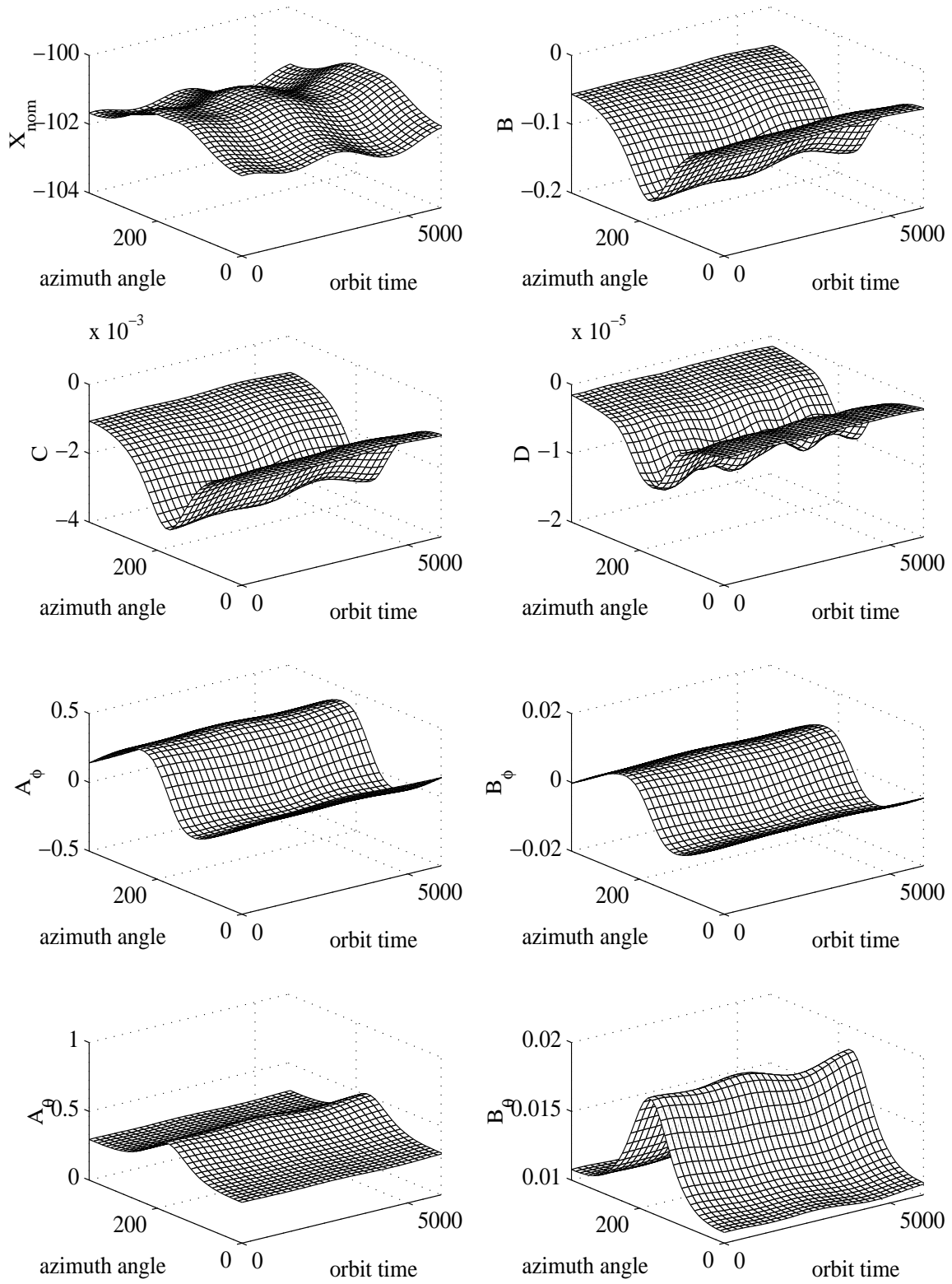


**Figure 5.** Plots showing the variation of some of the values stored in the X-table with orbit time and azimuth angle. These plots are for slice 5 of the inner beam and the nominal resolution mode.

**Table 2.** The maximum standard deviations for the inner 8 slices of the nominal resolution mode, both beams included. The standard deviations in slice center azimuth ( $\phi$ ) and elevation ( $\theta$ ) angles have been converted to meters to make them easier to comprehend.

parameter	QuikSCAT	ADEOS II
$X$ (dB)	.02	0.06
$\phi$ (meters)	75	110
$\theta$ (meters)	51	110

## 6. CONCLUSION

We have worked to develop an accurate, robust method for table driven  $\sigma^\circ$  retrieval for *SeaWinds*. The accuracy of the X-table has been verified by comparing the values of  $X$  and the slice centers retrieved from the table with those calculated independently by JPL. The results of all of the accuracy tests indicate that the table driven part of the ground data processing for *SeaWinds* will be accurate to within 0.1 dB for  $\sigma^\circ$  and 160 meters for the slice centers. After *QuikSCAT* is launched, further studies will be conducted to validate the accuracy of the X-table. The innovations developed as part of this algorithm may be of interest in processing data from other remote sensing systems.

## REFERENCES

1. F. Ulaby, R. Moore, and A. Fung, *Microwave Remote Sensing: Active and Passive*, vol. 2, Artech House, Inc., Norwood, Massachusetts, 1986.
2. M. Spencer, C. Wu, and D. Long, "Improved resolution backscatter measurements with the SeaWinds pencil-beam scatterometer," in *IEEE Trans. on Geosci. and Rem. Sens.*, 1999.
3. I. Ashcraft, "Correcting X for topography," Tech. Rep. MERS 98-07, Brigham Young University, Microwave Earth Remote Sensing Laboratory, December 1998.
4. A. Anderson, "Tabularizing the slice center location for Seawinds," Tech. Rep. MERS 98-05, Brigham Young University, Microwave Earth Remote Sensing Laboratory, July 1998.
5. B. Jones, D. Long, I. Ashcraft, and A. Anderson, "Background an accuracy analysis of the Xfactor7 Table," Tech. Rep. MERS 99-01, Brigham Young University, Microwave Earth Remote Sensing Laboratory, January 1999.